Dynamic scaling of the structure function for spinodal decomposition in critical and non-critical mixtures of poly(vinyl acetate)–poly(methyl methacrylate)

Mo Song, Yuhui Huang and Guangmin Cong
Guangzhou Institute of Chemistry, Academia Sinica, Guangzhou P.O. Box 1122, P.R. China

and Haojiun Liang and Bingzheng Jiang
Changchun Institute of Applied Chemistry, Academia Sinica, Changchun 130022, P.R. China
(Received 30 May 1990; revised 30 October 1990; accepted 20 March 1991)

The dynamics of phase separation in a binary polymer blend of poly(vinyl acetate) with poly(methyl methacrylate) was investigated by using a time-resolved light-scattering technique. In the later stages of spinodal decomposition, a simple dynamic scaling law was found for the scattering function $S(q,t)(S(q,t) \sim I(q,t))$: $S(q,t)q_m^{-3}\tilde{S}(q/q_m)$. The scaling function determined experimentally was in good agreement with that predicted by Furukawa, $\tilde{S}(X) \sim X^2/(3+X^8)$ for critical concentration, and approximately in agreement with that predicted by Furukawa, $\tilde{S}(X) \sim X^2/(3+X^6)$ for non-critical mixtures. The light-scattering invariant shows that the later stages of the spinodal decomposition were undergoing domain ripening.

(Keywords: phase separation; scaling; structure function; light scattering; poly(vinyl acetate); poly(methyl methacrylate))

INTRODUCTION

The dynamics of phase separation by spinodal decomposition in a binary polymer mixture is an interesting subject because the study of the spinodal decomposition process is important for designing and controlling the structure and properties of multicomponent polymer materials and for understanding non-equilibrium dynamic processes in general involving cooperative phenomena and self-organization of systems.

A number of experimental studies have reported the processes of the spinodal decomposition. There have been significant advances in the understanding of spinodal decomposition in polymer mixtures[1–7]. Since the work of Van Aartsen[8], who made the first attempt to apply the linearized Cahn theory[9] to a polymer solution, polymer–polymer blends have proved an attractive class of materials with which to investigate phase-separation dynamics. Owing to their molecular weight, the study of spinodal decomposition is easier than for alloy systems in the early stages. Polymer blends are characterized by mean-field behaviour, which facilitates the application of Cahn's theory.

In the early stages of spinodal decomposition, the growth in amplitude of dominant concentration fluctuations primarily takes place with no change in size, as Cahn's theory predicts[9,10]. In the transition from early to late stages, both the size and amplitude of concentration fluctuations grow, and in the final stage the change in structure with time involves size growth only[11]. The structure of the microphase changes involves 'self-similarity'[12]. Therefore, the time evolution of the characteristic length of the structure is expected to follow a power law, so that I_m and q_m, which characterize the maximum scattered intensity and the characteristic size (q_m^{-1}), respectively, obey the power laws:

$$q_m(t) \sim t^{-a} \tag{1}$$

$$I_m(t) \sim t^{\phi} \tag{2}$$

with

$$\phi/a = d \tag{3}$$

where d is the spatial dimension.

The self-similarity of phase structures in the later stages of spinodal decomposition requires a scaling law for the structure function $S(q,t)$ predicted by Furukawa[13]

$$S(q,t) \sim q_m^{-d}(t)\tilde{S}(X) \tag{4}$$

where $\tilde{S}(X)$ is a universal function independent of time t

$$\tilde{S}(X) \sim X^2/(y/2 + X^{2+y}) \tag{5}$$

$$X = q/q_m \tag{6}$$

$$\tilde{S}(X) \sim \begin{cases} X^2 & \text{for small } X \\ X^{-y} & \text{for large } X \end{cases} \tag{7}$$

where q is the scattering vector

$$q = 4\pi/\lambda \sin(\theta/2) \tag{8}$$

0032-3861/92/061293-06

The quantities λ and θ are the wavelength of light in the medium and the scattering angle, respectively, and $y = 2d$ for the critical concentration, but $d + 1$ for the non-critical concentration.

This paper focuses attention on the dynamic scaling behaviour of the structure function of spinodal decomposition in a binary polymer mixture of poly(vinyl acetate) with poly(methyl methacrylate) (PVAc–PMMA).

EXPERIMENTAL

PMMA ($M_w = 1.98 \times 10^5$, $M_n = 7.7 \times 10^4$) and PVAc ($M_w = 2.6 \times 10^6$, $M_n = 8.0 \times 10^5$) were from commercial products from Polymer Science Ltd (USA). For cloud-point and light-scattering experiments, the blends were prepared by dissolving in chloroform as a common solvent. The concentration was 3 wt%. The blend samples were cast on cover glass and the solvent was allowed to evaporate slowly. The films were kept under vacuum at 50°C until no further weight loss was observed.

A 2 mW He–Ne laser light source with a wavelength of 632.8 nm was used. The series of spinodal decomposition experiments were made in steps from 25°C to a two-phase region for various temperatures. A temperature controller with an accuracy of ± 0.2°C was used[14].

The relative scattered intensity was measured by a light-scattering technique and the relative scattered intensity profiles were normalized by the film thickness so that they could be compared. The scattered angle θ was corrected for turbidity[15] h

$$I_c(\theta) = I_d(\theta)\exp(hd/\cos\theta)\{hd(\cos^{-1}\theta - 1)\} \times \{\exp(hd(\cos^{-1}\theta - 1)) - 1\}^{-1} \quad (9)$$

where $I_c(\theta)$ and $I_d(\theta)$ are corrected and measured scattered intensity distributions, respectively, and d is the sample thickness. The corrected scattered intensity I_c was used for further analyses.

RESULTS AND DISCUSSION

Estimation of the phase behaviour of PMMA–PVAc is considered first. Casting from chloroform solution, all films of PMMA–PVAc blends with different compositions were optically clear. Even after annealing at 110°C for 24 h, they were transparent and no indication of phase separation was observed under an optical microscope. The blend films on the cover glass were placed on a hot plate and the temperature increased at a rate of 10 K min^{-1}. As the temperature increased, the films became opaque at which point we judged that the blend had entered the two-phase region in the phase diagram[16]. When the temperature had reached over 170°C, all of the films of various compositions became opaque. *Figure 1a* is the phase diagram for PMMA–PVAc blends. The results show that PMMA–PVAc exhibited a lower critical solution temperature (LCST). The solid curve is the binodal line and open points are spinodal. The spinodal points were determined dynamically by using time-resolved light-scattering. In the early stages of phase separation the scattered intensity increases exponentially with time t in the spinodal region[9]

$$I(q,t) = I(q,0)\exp(2R(q)t) \quad (10)$$

$$R(q) = D_{app}q^2 - 2KMq^4 \quad (11)$$

where M is the mobility constant, K is the coefficient

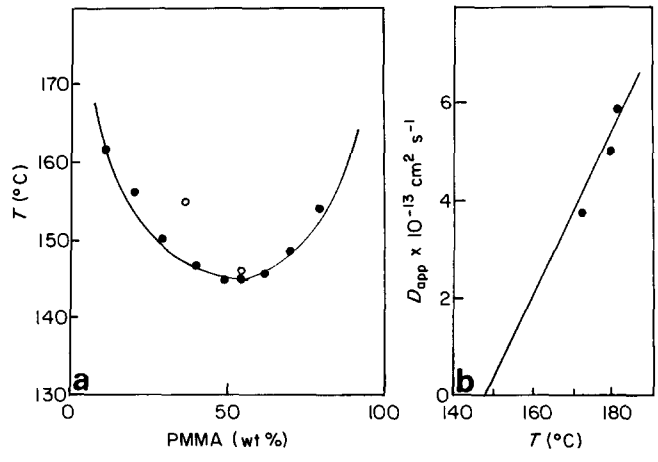

Figure 1 (a) The cloud-point curve and the spinodal point for PMMA–PVAc mixtures; (b) the temperature dependence of D_{app}

associated with gradient-free energy density and D_{app} is the apparent diffusion coefficient. The spinodal point was achieved by measuring the apparent diffusion coefficient D_{app} as a function of temperature. The spinodal temperature was determined as the temperature at which D_{app} became zero. This result for PMMA–PVAc (55:45 by weight) is shown in *Figure 1b*. For that mixture the critical composition of PMMA, ϕ_c, and critical temperature, T_c, are

$$\phi_c = 0.55 \qquad T_c = 146°C$$

The cloud-point curve was skew. Generally, miscible polymers tend to phase separation at elevated temperatures. This LCST behaviour is typical for miscible polymer blends. As shown below, the phase separation near a LCST is entropy-driven. As for our results obtained by using d.s.c. and *FT*i.r.[17], it gave information about miscible blends for PMMA–PVAc casting from chloroform.

Typical time evolution for scattering curves for the PMMA–PVAc critical composition are shown in *Figure 2* for $T = 180.6$°C. When the blend undergoes phase separation, a clear scattering maximum develops at a particular angle. As phase separation proceeds, this scattering maximum moves to lower scattering angles associated with phase growth, while the scattered intensity increases with phase separation time t.

Detailed analyses from our experimental results showed that the phase-separation processes can be described by a three-stage model: early, intermediate and late. The early stage is accounted for by Cahn's theory, yielding initial correlation lengths and effects of diffusion coefficients in quantitative agreement with mean-field predictions. The scattered intensity increases exponentially with time (i.e. according to equation (9)). The results for PMMA–PVAc (55:45 by weight) at 177.4°C are shown in *Figure 3*. Phase ripening and non-linear effects mark the beginning of the intermediate stage, where the amplitude of the concentration fluctuations and the wavelength of the dominant Fourier mode of fluctuation increase with time. This results in a non-linear increase of scattered intensity, clearly shown in *Figure 3* after 15 min. As the composition fluctuation amplitude approaches equilibrium values, the spinodal decomposition process enters the late stage, where the structures occurring at different times have the 'self-similarity' that

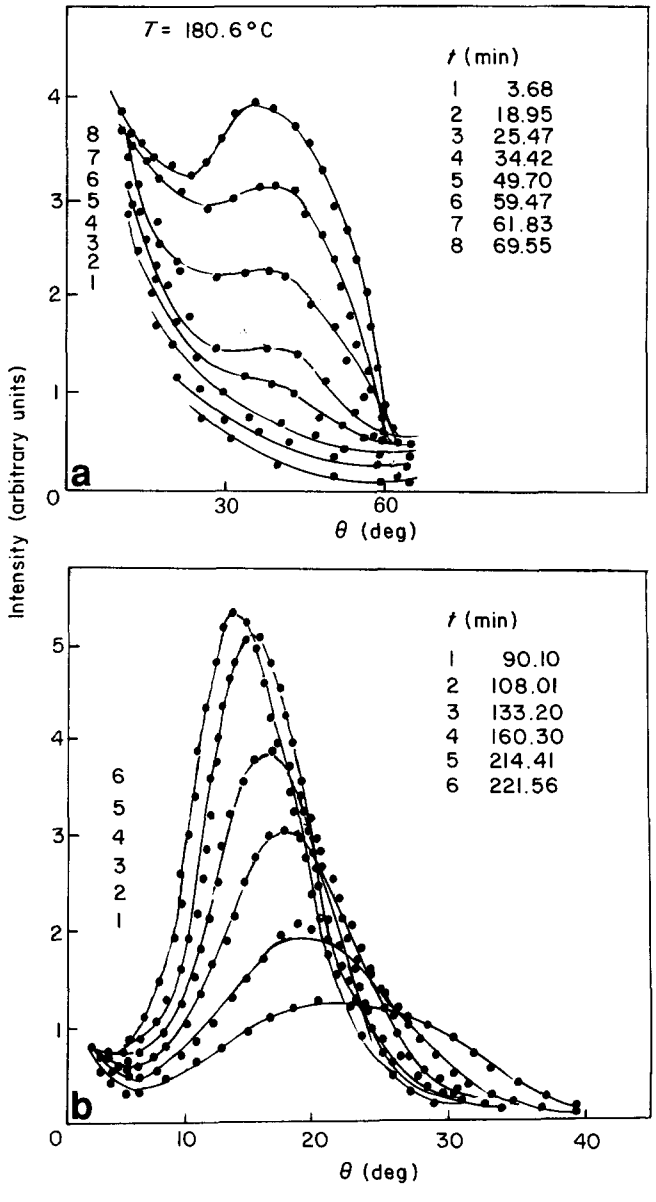

Figure 2 Time evolution of light-scattering profiles during isothermal phase separation at 180.6°C for the critical concentration for the PMMA–PVAc mixture

can be characterized by fractal theory[18], and dynamic scaling of the structure function can be effected, which will be discussed later.

The scaling behaviour of $q_m(t)$ and $I_m(t)$ has been fully discussed in another paper[18]. Here we are concerned with the scaling of the scattering profiles $I(q, t)$. *Figures 4* and *5* show the scaled structure factor $F(X)$ at 180.6, 177.4, 172.0°C for critical concentration, and at 184.2 and 175.0°C for non-critical concentration, respectively, where $F(X)$ is defined as

$$F(X) = q_m^3 I(q/q_m) \tag{12}$$

with X defined in equation (6). As can be seen in *Figures 4* and *5*, reasonably superimposed master curves were obtained for all T-jumps in the late stage of the spinodal phase separation, suggesting that dynamic self-similarity is preserved throughout the phase-separation process. In the later stages of spinodal decomposition, the growth of the phase-separation domains satisfies the dynamic scaling hypothesis with the single length parameter[11,19] $q_m(t)^{-1}$. Hence the domains grow with dynamic self-similarity. Dynamic scaling of the structure function of spinodal phase separation in polymer blends has also been found for other physical systems[20,21].

The experimentally scaled structure factor $\tilde{S}(X)$ was compared with the theoretically scaled structure factor obtained by Furukawa[13] (see equation (4)). To facilitate the comparison, the scaled structure factors are normalized by[12]

$$\tilde{S}(X)_{\text{expt}} = q_m^3 I(q, t) \Big/ \int_{X_{\min}}^{X_{\max}} q^2 I(q, t)\, dq \tag{13}$$

$$\tilde{S}(X)_{\text{theor}} = \tilde{S}(X) \Big/ \int_{X_{\min}}^{X_{\max}} X^2 \tilde{S}(X)\, dX \tag{14}$$

The theoretical values of $\tilde{S}(X)$ were calculated from the scaling function $\tilde{S}(X)$ for non-critical and critical mixtures in three-dimensional space:

$$\tilde{S}(X) \sim X^2/(3 + X^8) \quad \text{for critical} \tag{15}$$

$$\tilde{S}(X) \sim X^2/(2 + X^6) \quad \text{for non-critical} \tag{16}$$

Figures 6 and *7* show the normalized scaled structure factor $\tilde{S}(X)$ thus determined for the unmixing at 180.6°C and 177.4°C for critical concentration, and at 184.2 and 175.0°C for non-critical concentration, respectively. The solid curves are the theoretical ones. The results clearly showed that in the intermediate stage $\tilde{S}(X)$ itself depends on time and $\tilde{S}(X)$ obtained at different times do not fall onto the theoretical curve. In this stage the phase separation process cannot be scaled with a single length parameter, q_m^{-1}, because concentration fluctuation is changing with time; in the late stage, the amplitude of fluctuations between the two phases reaches the equilibrium value, such that $\tilde{S}(X)$ itself becomes time-independent. Meanwhile, it was found that the scaling law of the structure function given by equation

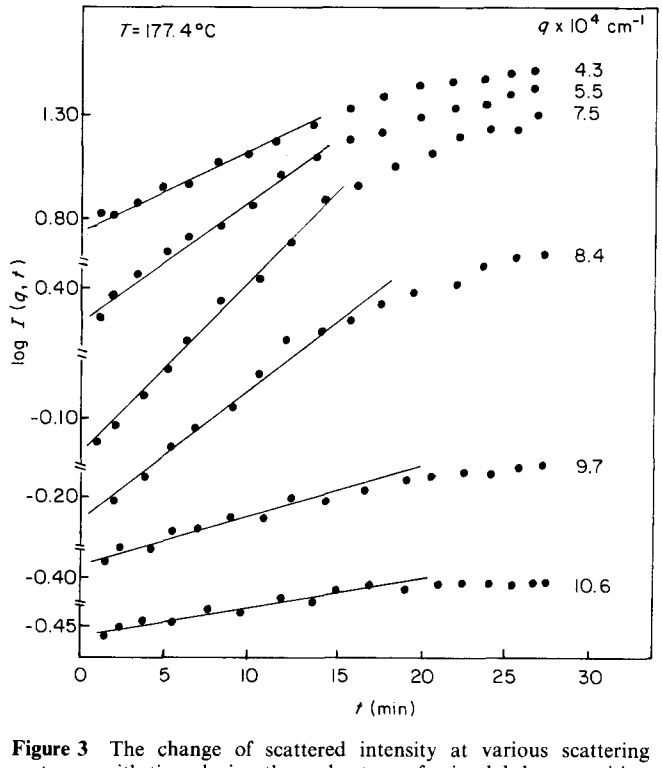

Figure 3 The change of scattered intensity at various scattering vectors q with time during the early stage of spinodal decomposition at 177.4°C for the critical mixture

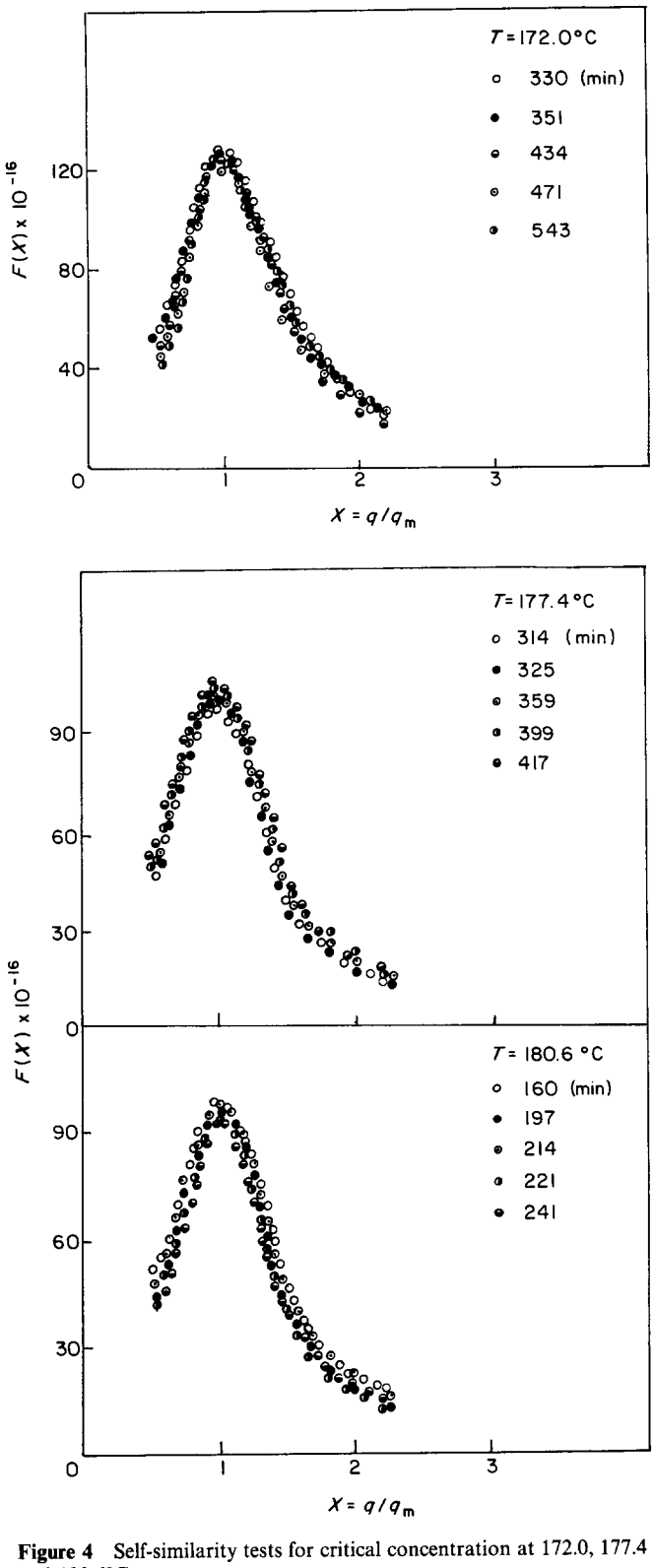

Figure 4 Self-similarity tests for critical concentration at 172.0, 177.4 and 180.6°C

(15) is satisfied for the critical concentration at 180.6°C, but the scaling law is only approximately satisfied at 177.4°C. For the non-critical concentration, the experimental data gradually change with time t to form a broader peak and tail so that the scaling law is also only approximately satisfied.

The asymptotic behaviour of the experimentally and theoretically scaled structure factors $\tilde{S}(X)_{\text{expt}}$ and $\tilde{S}(X)_{\text{theor}}$ at small X and large X are compared in *Figures*

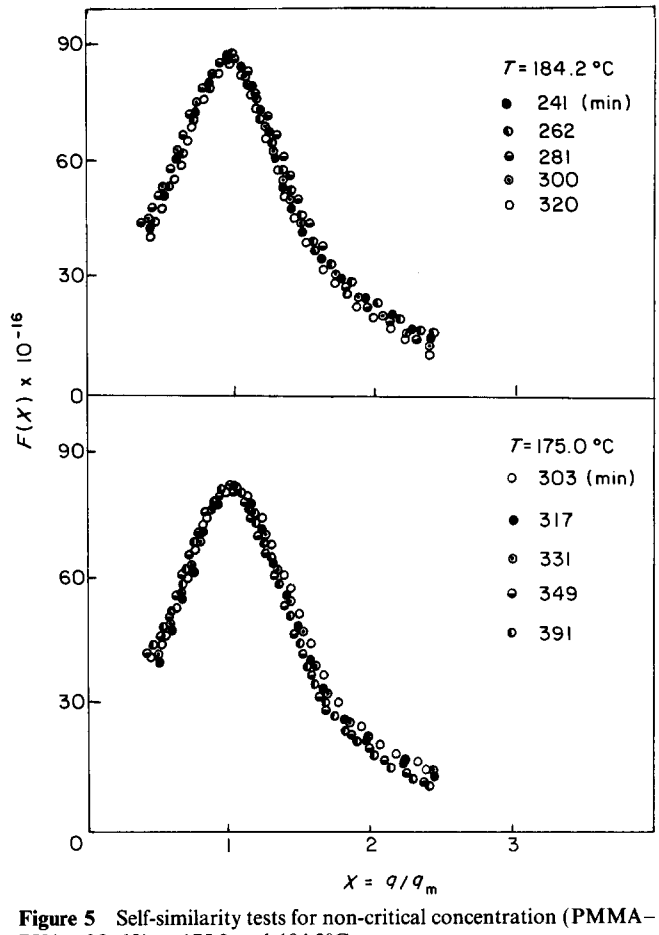

Figure 5 Self-similarity tests for non-critical concentration (PMMA–PVAc, 35:65) at 175.0 and 184.2°C

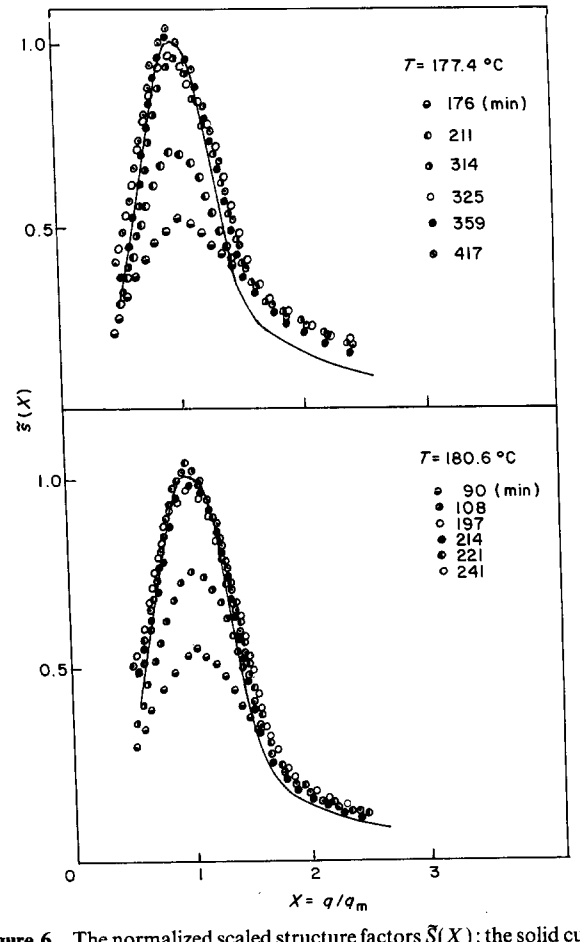

Figure 6 The normalized scaled structure factors $\tilde{S}(X)$: the solid curve is from theory (PMMA–PVAc, 55:45 for $T = 177.4$ and 180.6°C)

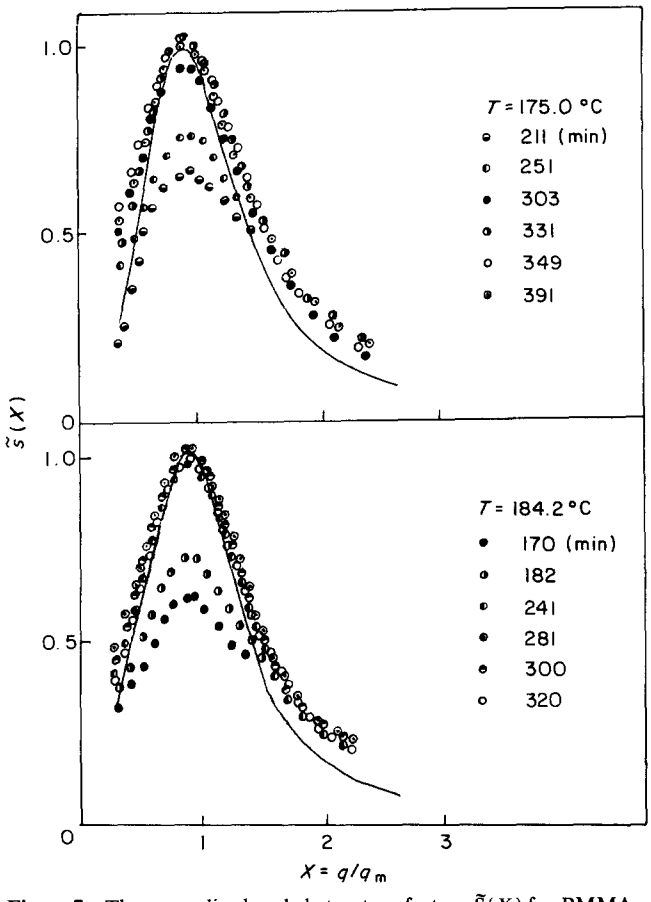

Figure 7 The normalized scaled structure factors $\tilde{S}(X)$ for PMMA–PVAc (35:65) system at 175.0 and 184.2°C: the solid curve is from theory

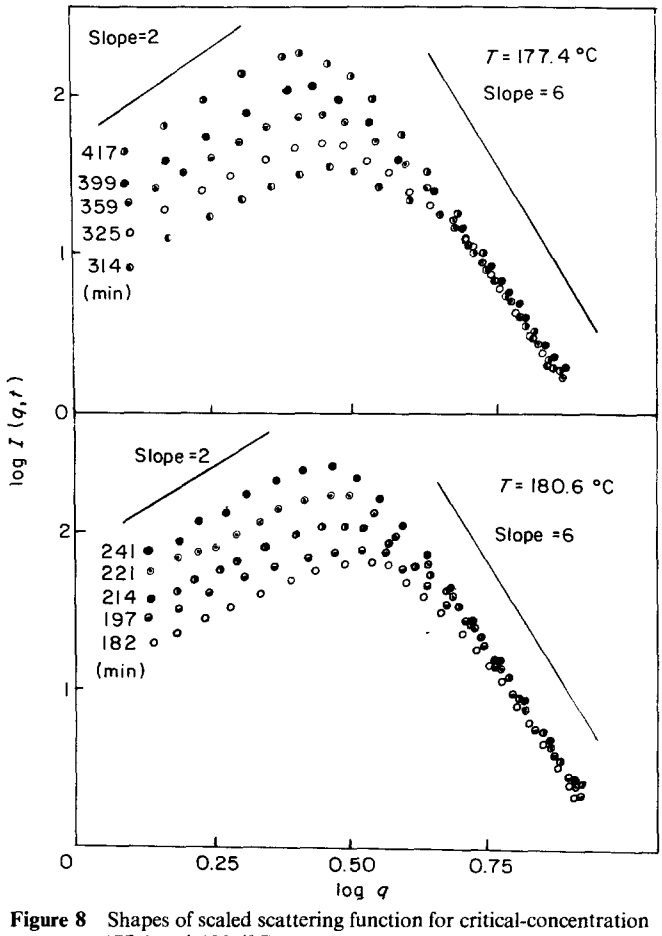

Figure 8 Shapes of scaled scattering function for critical-concentration system at 177.4 and 180.6°C

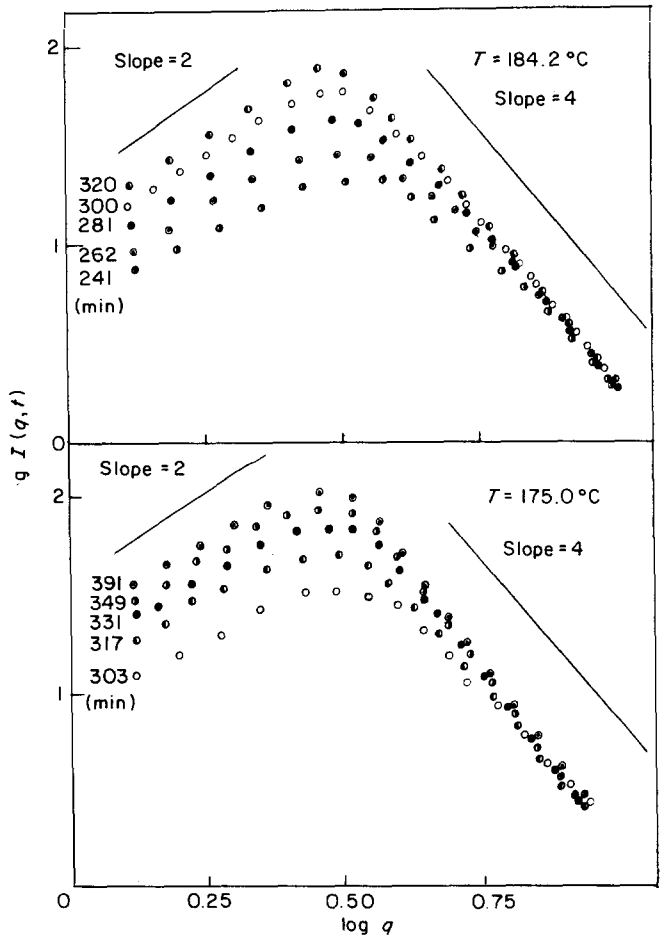

Figure 9 Shapes of scaled scattering function for 35:65 PMMA–PVAc blends at 175.0 and 184.2°C

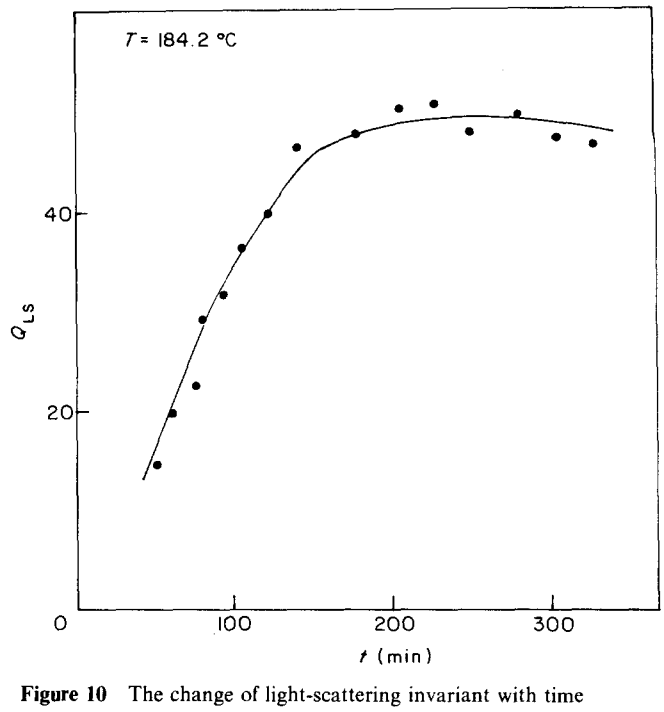

Figure 10 The change of light-scattering invariant with time

8 and *9* for various temperatures for critical and non-critical concentration, respectively. The results showed, at $q > q_m$, $\tilde{S}(X)$ is approximately proportional to X^{-4} and X^{-6} for non-critical and critical concentrations, respectively. The scattering function in the

Porod law region is given by[22]

$$I(q) \sim q^{-4}(1 - q^{-2}/R_m^2 + \ldots) \qquad (17)$$

where R_m is the mean radius of the wavy interface; $I(q) \sim q^{-4}$ for the ideal two-phase structure. However, for $I(q) \sim q^{-6}$, it does not correlate well. Ohyama *et al.*[23] gave a different result for critical concentration.

To determine whether an unmixing system was undergoing domain ripening, the light-scattering invariant was observed as a function of time for non-critical concentration at 184.2°C, as shown in *Figure 10*. The light-scattering invariant was defined by[24]

$$Q_{LS} = \int_{q_{min}}^{q_{max}} q^2 I(q)\, dq \qquad (18)$$

The light-scattering invariant can be expressed by[24]

$$Q_{LS} = (32\pi^6/\lambda_0)\phi_1\phi_2(a_1 - a_2)^2 \qquad (19)$$

where ϕ_1, ϕ_2, a_1, a_2 are the volume fractions and polarizabilities of the two phases. If domain ripening is the only process occurring, both $\phi_1\phi_2$ and $(a_1 - a_2)^2$ remain constant, and thus Q_{LS} also remains constant. Our result showed clearly that the blend was undergoing domain ripening. It should be worth noting that the time at which the light-scattering invariant is constant is nearly the same as the time at which the scaling law of the structure function holds.

Recently, the fractal behaviour of ramified phase structure by spinodal decomposition has been studied[18,25]. It was found that fractal concepts[26] can describe the behaviour of phase structure by spinodal phase separation. Both mass and surface fractal for ramified domains may cause dynamic scaling of the structure function. We are continuing to study that problem.

REFERENCES

1 Binder, K. *J. Chem. Phys.* 1983, **79**, 6387
2 deGennes, P. G. *J. Chem. Phys.* 1980, **72**, 4756
3 Gelless, R. and Frank, C. W. *Macromolecules* 1982, **15**, 1486
4 Hashimoto, T., Sasaki, M. and Kawai, H. *Macromolecules* 1984, **17**, 2812
5 Hashimoto, T. and Izumitani, T. *Polym. Prepr., Am. Chem. Soc. Div. Polym. Chem.* 1985, **26**, 66
6 Sato, T. and Han, C. C. *J. Chem. Phys.* 1988, **88**, 2057
7 Kyu, T. and Saldanha, J. M. *Macromolecules* 1988, **21**, 1021
8 Van Aartsen, J. *Eur. Polym. J.* 1970, **6**, 919
9 Cahn, J. W. and Hilliard, J. E. *J. Chem. Phys.* 1958, **28**, 258
10 Higgins, J. S., Fruitwala, H. A. and Tomlins, P. E. *Brit. Polym. J.* 1989, **21**, 247
11 Hashimoto, T., Itakura, M. and Shimidzu, N. *J. Chem. Phys.* 1986, **85**, 6773
12 Hashimoto, T., Itakura, M. and Hasegawa, H. *J. Chem. Phys.* 1986, **85**, 6118
13 Furukawa, H. *Adv. Phys.* 1985, **34**, 703
14 Song, M., Liang, H. and Jiang, B. *Acta Polymerica Sinica* 1990, **2**, 176
15 Stein, R. S. and Keane, J. J. *J. Polym. Sci.* 1955, **17**, 21
16 Paul, D. R. *et al. Macromolecules* 1977, **4**, 681
17 Song, M. and Long, F. *Eur. Polym. J.* 1991, **27**, 983
18 Song, M., Huang, Y. and Cong, G. *Eur. Polym. J.* (in press)
19 Yang, J. and Kyu, T. *Macromolecules* 1990, **23**, 182
20 Hennion, M., Ronzaud, D. and Guyot, P. *Acta Metall.* 1982, **30**, 599
21 Katano, S. and Iizumi, M. *Phys. Rev. Lett.* 1984, **83**, 3694
22 Tomita, H. *Progr. Theor. Phys.* 1986, **75**, 482
23 Ohyama, Y., Kinoshita, S., Takahashi, M. and Nose, T. *Rep. Progr. Polym. Phys. Jpn.* 1984, **27**, 503
24 Gilmer, J., Goldstein, N. and Stein, R. S. *J. Polym. Sci., Polym. Phys. Edn.* 1982, **20**, 2219
25 Song, M. *et al. Polym. Bull.* 1991, **25**, 515
26 Mandelbrot, B. B. 'The Fractal Geometry of Nature', Freeman, New York, USA, 1982